

1 **ASYMPTOTIC EXPANSIONS OF EVOLUTION EQUATIONS WITH**
2 **FAST VOLATILITY**

3 SAM D. HOWISON*, CHRISTOPH REISINGER*, RONNIE SIRCAR†, AND ZHENRU
4 WANG*

5 **Abstract.** We study Kolmogorov forward equations (KFE) and Zakai equations for diffusion
6 processes with a fast mean-reverting stochastic volatility component. In the case of the KFE, a
7 parabolic PDE in divergence form, we perform a matched asymptotic expansion up to first order in
8 the small mean-reversion time. The solutions are expressed in terms of suitable PDEs with coefficients
9 averaged over the ergodic distribution, in the spirit of extensive earlier work on the backward equation
10 (see *J.-P. Fouque et al, CUP, 2011*). We then construct a sequence of approximations to the Zakai
11 equation, a parabolic stochastic PDE (SPDE), and verify numerically for the first two terms weak
12 convergence order half and order one, respectively, in the mean-reversion parameter. To this end, we
13 give a novel numerical scheme for the original two-dimensional SPDE, which is robust in the small
14 parameter regime, and compare derived functionals of marginals against those approximated by the
15 solution of a sequence of homogenised one-dimensional SPDEs.

16 **Key words.** matched asymptotic expansions, stochastic volatility, fast mean-reversion, forward
17 Kolmogorov equation, Zakai equation

18 **AMS subject classifications.** 60H15, 35R60, 35C20, 65C30, 65M99

19 **1. Introduction.** In this work, we consider processes of the form

$$\begin{aligned}
 (1.1) \quad dX_t &= \mu(X_t, Y_t) dt + \sigma(Y_t) \left(\rho_x dW_t^x + \sqrt{1 - \rho_x^2} dW_t^{x,1} \right), \quad X_0 = x_0, \\
 dY_t &= \frac{\kappa}{\epsilon} (m - Y_t) dt + \frac{g(Y_t)}{\sqrt{\epsilon}} \left(\rho_y dW_t^y + \sqrt{1 - \rho_y^2} dW_t^{y,1} \right), \quad Y_0 = y_0,
 \end{aligned}$$

21 where $(W^x, W^y, W^{x,1}, W^{y,1})$ is a four-dimensional standard Brownian motion, W^x
22 and W^y have correlation $\rho \in (-1, 1)$, while $W^{x,1}, W^{y,1}$ are independent of each other
23 and of (W^x, W^y) ; $x_0, y_0, m \in \mathbb{R}, \rho_x, \rho_y \in (-1, 1), \epsilon, \kappa > 0$ are all constant; $\mu : \mathbb{R} \times \mathbb{R} \rightarrow$
24 \mathbb{R} and $\sigma, g : \mathbb{R} \rightarrow \mathbb{R}_+$ given functions. For ease of notation, we introduce $\rho_{xy} = \rho_x \rho_y \rho$.

25 We will study the marginal distribution of (X_t, Y_t) at t , and the distribution of
26 (X_t, Y_t) conditional on the natural filtration $\mathcal{F}_t^{x,y}$ of $W = (W^x, W^y)$ at time t , which is
27 the reason for writing the Brownian driver in the decomposed way above. Specifically,
28 we are interested in the setting of small ϵ , a characteristic, dimensionless reversion time
29 of the Y -process to its mean m , and will derive equations for asymptotic expansions of
30 the probability density function (PDF) and the conditional PDF. The former leads us
31 to derive matched asymptotic expansions of the corresponding Kolmogorov *forward*
32 equation (KFE, or Fokker–Planck equation), a two-dimensional parabolic PDE in
33 divergence form, while the latter leads to expansions of a Zakai-type equation, a
34 parabolic stochastic PDE (SPDE).

35 Models of the form (1.1) are used abundantly in financial engineering, where X
36 describes the log price of a financial asset and $\sigma(Y_t)$ is its instantaneous (stochastic)
37 volatility at time t . The presence of multiple time scales in market data has been doc-
38 umented extensively in the literature; see, e.g., [11, 10], and especially the monograph
39 [12] and the references therein. For higher order expansions with a refined boundary

*Mathematical Institute, University of Oxford, United Kingdom (howison@maths.ox.ac.uk,
christoph.reisinger@maths.ox.ac.uk, zrwang1128@gmail.com)

†ORFE Department, Princeton University, Princeton, NJ, USA (sircar@princeton.edu)

layer analysis close to expiry we refer to [19] and [8], also [5] for a convergence analysis. The expansion at the level of the underlying stochastic processes is analysed in [13] (see also the earlier discussion in the conclusions of [19]). Among more recent works, [2] performs joint asymptotic expansions of optimal investment models with fast volatility and small transaction costs, and [7] demonstrates a multiscale analysis of portfolio optimisation strategies under fast and slow volatilities.

The above Kolmogorov *backward* equations (KBE) are in non-divergence form and typically have regular (i.e., continuous) terminal data, while the Kolmogorov *forward* equations (KFE) studied here are in divergence form with Dirac delta initial data. Specifically, we will consider the model where μ is constant, and $g = \nu\sqrt{2}$ for constant ν , that is where Y an Ornstein–Uhlenbeck process, with unique ergodic distribution $\mathcal{N}(m, \nu^2)$.¹ In this case, the KFE is

$$\begin{aligned} \partial_t p^\epsilon &= \frac{1}{\epsilon} \left(\nu^2 \partial_{yy} p^\epsilon - \kappa \partial_y ((m - y) p^\epsilon) \right) + \left(\frac{1}{2} \sigma^2(y) \partial_{xx} p^\epsilon - \mu \partial_x p^\epsilon \right) \\ &+ \frac{1}{\sqrt{\epsilon}} \rho_{xy} \nu \sqrt{2} \partial_y (g(y) \partial_x p^\epsilon), \\ p^\epsilon(0, x, y) &= \delta(x - x_0) \otimes \delta(y - y_0). \end{aligned} \tag{1.2}$$

Apart from being of interest in its own right, the analysis of the forward PDE serves as preparation for that of the Zakai SPDE

$$\begin{aligned} du^\epsilon &= \frac{1}{\epsilon} \left(\nu^2 \partial_{yy} u^\epsilon - \kappa \partial_y ((m - y) u^\epsilon) \right) dt + \left(\frac{1}{2} \sigma^2(y) \partial_{xx} u^\epsilon - \mu \partial_x u^\epsilon \right) dt \\ &+ \frac{1}{\sqrt{\epsilon}} \rho_{xy} \nu \sqrt{2} \partial_y (g(y) \partial_x u^\epsilon) dt + \rho_x \sigma(y) \partial_x u^\epsilon dW_t^x + \rho_y \frac{\sqrt{2}\nu}{\sqrt{\epsilon}} \partial_y u^\epsilon dW_t^y, \\ u^\epsilon(0, x, y) &= \delta(x - x_0) \otimes \delta(y - y_0). \end{aligned} \tag{1.3}$$

There are at least two motivations for studying (1.3). First, by general filtering theory (see, e.g., [1, Section 3.5]), the solution u^ϵ is the density (if it exists) of the conditional law of (X_t, Y_t) given observation of (W^x, W^y) up to time t . Second, it is the limit empirical measure of a large number N of independent realisations of (1.1), with independent (idiosyncratic) noise terms $W_t^{x,i}, W_t^{y,i}$, for $i = 1, \dots, N$, replacing $W_t^{x,1}, W_t^{y,1}$, but all with the same common noise W_t^x, W_t^y (see, e.g., [20]).

This limiting equation has been used to describe the behaviour of large pools of defaultable financial entities, where the process X is replaced by one absorbed at 0 (a ‘default boundary’), and the absorption of mass is interpreted as a loss to the financial system. The case of constant σ is analysed in [4] and applications to credit derivative markets are given. For a (nonlinear) SPDE model for a large pool limit of a default intensity-based credit model see e.g. [14]. More recently, an extension of the basic model in [4] to stochastic volatilities is given in [16, 17]. See also [21, 22] for different applications involving filtering of hidden Markov models with fast mean-reverting states.

We will focus particularly on the regime of small ϵ , as motivated by the empirical evidence cited above. In practical applications, one is predominantly interested in the behaviour of X , and in Y only in as much as it affects the dynamics of X . For instance, in credit risk, it is the firm log value process X which directly affects loss distributions. It is therefore desirable to derive simplified homogenised equations which allow for

¹The factor $\sqrt{2}$ is chosen to ensure the ergodic distribution has a more standard normal form, consistent with the literature (see [9, 12]).

76 more efficient analytical or numerical solutions by reducing the dimensionality of
 77 the PDE or SPDE. The numerical approximation of the original two-dimensional
 78 KFE or Zakai SPDE, especially, is more costly computationally than that of the one-
 79 dimensional analogue with deterministic (e.g., constant) volatility. This is exacerbated
 80 by the presence of multiple scales, which may require a fine time mesh and fine spatial
 81 mesh in the second dimension for the stable resolution of the fast component for small
 82 parameter ϵ .

83 By expansion in ϵ , we will approximate p^ϵ and u^ϵ by sequences of KFEs and
 84 Zakai SPDEs, respectively, which have the advantageous feature that the fast varying
 85 volatility is replaced by its ergodic average in the differential operator, and, in the
 86 case of the SPDE, the driving noise term. Moreover, if only functionals of X (and not
 87 Y) are required, these can be computed by the solution of one-dimensional (S)PDEs,
 88 leading to an effective dimension reduction and complexity advantage.

89 In the context of (1.1), [18] consider the case of $\mu(X_t, Y_t) = r - \sigma^2(Y_t)/2$, for
 90 constant r .² Under certain recurrence properties of the diffusion Y , and for $\rho_{xy} = 0$,
 91 it is shown that as $\epsilon \rightarrow 0$, the stopped version of X converges in distribution to a
 92 process X^* which satisfies

$$93 \quad (1.4) \quad dX_t^* = (r - \langle \sigma^2 \rangle / 2) dt + \sqrt{\langle \sigma^2 \rangle} \left(\rho dW_t^x + \sqrt{1 - \rho^2} dW_t^{x,1} \right), \quad X_0 = x_0,$$

94 where $\langle \sigma^2 \rangle$ is the expectation of $\sigma^2(\cdot)$ under the invariant distribution of Y .

95 Moreover, weak limits of u^ϵ are shown to satisfy the SPDE

$$96 \quad (1.5) \quad du^* = \left(\frac{1}{2} \langle \sigma^2 \rangle \partial_{xx} u^* - (r - \langle \sigma^2 \rangle / 2) \partial_x u^* \right) dt + \rho_x \langle \sigma \rangle \partial_x u^* dW_t^x,$$

97 where $\langle \sigma \rangle$ is the expectation of $\sigma(\cdot)$ under the invariant distribution of Y .

98 We note that [18] allow for more general g in (1.1) than for the Ornstein–
 99 Uhlenbeck (O–U) process considered here. On the other hand, we want to avoid the
 100 assumption $\rho_{xy} = 0$, as the correlation between volatility and stock is an important
 101 parameter influencing the dynamic behaviour of stock price models. In particular, it
 102 is used to match the implied volatility skew in derivatives markets, while a realistic
 103 dependence of increments of the two processes is key for successful hedging. To deal
 104 with this dependence, we make more specific assumptions on the volatility process,
 105 and restrict ourselves to O–U processes, which will allow a decomposition of Y such
 106 that the SPDE is driven purely by the slow component, while fast-mean-reverting
 107 term appears explicitly in the coefficients. This helps with the construction of cor-
 108 rection terms for a higher order expansion of the SPDE. However the function σ is
 109 general up to technical restrictions.

110 The main contributions and outline of the present paper are the following:

- 111 • a matched asymptotic expansion solution of the KFE (1.2) for small ϵ , iden-
 112 tifying the boundary layer for small t and deriving the expansion up to order
 113 1 for general t (Section 2);
- 114 • the heuristic derivation of a one-dimensional SPDE for a first-order correction
 115 to (1.5) in ϵ (Section 3);
- 116 • numerical verification of the SPDE expansion orders (in Section 5) by novel
 117 numerical schemes for (1.3) and related SPDEs, with a proof of unconditional
 118 stability independent of ϵ (Section 4).

119 2. Perturbation analysis of the KFE.

²In fact, [18] allow that r and other (constant) model parameters are sampled randomly.

120 **2.1. Set-up and preliminaries.** We derive an expansion for the transition
 121 density function of a stochastic volatility process (X, Y) satisfying (1.1) with $g = \nu\sqrt{2}$
 122 for constant ν , as the dimensionless parameter $\epsilon \rightarrow 0^+$. We assume for simplicity that
 123 σ is bounded away from zero, such that the process X takes values on all of \mathbb{R} (as
 124 does the O–U process Y).

125 The transition density $p^\epsilon(t_0, x_0, y_0; t, x, y)$ of (X, Y) satisfies the forward Kol-
 126 mogorov equation (in the variables t, x, y)

$$127 \quad (2.1) \quad \partial_t p^\epsilon - \left(\frac{1}{\epsilon} \mathcal{L}_0^* + \frac{1}{\sqrt{\epsilon}} \mathcal{L}_1^* + \mathcal{L}_2^* \right) p^\epsilon = 0,$$

128 with the initial condition

$$129 \quad (2.2) \quad p^\epsilon(t_0, x_0, y_0; t_0, x, y) = \delta(x - x_0) \otimes \delta(y - y_0).$$

130 Here the operators \mathcal{L}_i and their adjoints \mathcal{L}_i^* are defined by

$$131 \quad (2.3) \quad \mathcal{L}_0 \cdot = \nu^2 \partial_{yy} \cdot + \kappa(m - y) \partial_y \cdot, \quad \mathcal{L}_0^* \cdot = \nu^2 \partial_{yy} \cdot - \kappa \partial_y ((m - y) \cdot),$$

$$132 \quad (2.4) \quad \mathcal{L}_1 \cdot = \rho_{xy} \nu \sqrt{2} \sigma(y) \partial_{xy} \cdot, \quad \mathcal{L}_1^* \cdot = \rho_{xy} \nu \sqrt{2} \partial_x \partial_y (\sigma(y) \cdot),$$

$$133 \quad (2.5) \quad \mathcal{L}_2 \cdot = \frac{1}{2} \sigma^2(y) \partial_{xx} \cdot + \mu(x, y) \partial_x \cdot, \quad \mathcal{L}_2^* \cdot = \frac{1}{2} \sigma^2(y) \partial_{xx} \cdot - \partial_x (\mu(x, y) \cdot).$$

135 We set $t_0 = 0$ for simplicity. We denote by Φ^Y the probability density function
 136 (PDF) of the ergodic distribution of Y ,

$$137 \quad (2.6) \quad \Phi^Y(y) = \frac{1}{\sqrt{2\pi\nu^2/\kappa}} e^{-\kappa(y-m)^2/2\nu^2}.$$

138 We shall frequently average functions of y with respect to the measure $\Phi^Y(y) dy$ and
 139 we use the notation $\langle \cdot \rangle = \langle \cdot, \Phi^Y \rangle$ for this average, where we denote by $\langle \cdot, \cdot \rangle$ the
 140 usual inner product on $L^2(\mathbb{R})$.

141 In what follows we shall repeatedly seek solutions of equations of the form

$$142 \quad (2.7) \quad -\mathcal{L}_0^* u(y) = h(y), \quad -\infty < y < \infty,$$

143 for some given h , that are integrable on \mathbb{R} . We note immediately that

$$144 \quad -\mathcal{L}_0^* \Phi^Y = 0, \quad -\mathcal{L}_0^* \left(\Phi^Y(y) \int^y \frac{ds}{\Phi^Y(s)} \right) = 0,$$

145 so that these functions span the null space of \mathcal{L}_0^* . However, integration by parts shows
 146 that, as $y \rightarrow \infty$,

$$147 \quad \int^y \frac{ds}{\Phi^Y(s)} = \text{constant} \times \int^y e^{\kappa(s-m)^2/2\nu^2} ds$$

$$148 \quad \sim \text{constant} \times \frac{e^{\kappa(y-m)^2/2\nu^2}}{y - m} (1 + O(1/y^2)),$$

150 and hence the function $\Phi^Y(y) \int^y ds/\Phi^Y(s)$ is not integrable. We shall use this fact
 151 to eliminate this solution at several points below.

152 The null space of $-\mathcal{L}_0$ is spanned by 1 and $e^{\kappa(y-m)^2/2\nu^2}$, the latter of these being
 153 irrelevant because of its growth at infinity (it is not even integrable against $\Phi^Y(y)$).

154 It follows from the Fredholm Alternative that integrable solutions of (2.7) only exist
 155 when the right-hand side satisfies the solvability condition of being orthogonal to
 156 (relevant, ie bounded) solutions of the homogeneous adjoint equation. That is, from

$$157 \quad \langle 1, h \rangle = \langle 1, -\mathcal{L}_0^* u \rangle = \langle -\mathcal{L}_0 1, u \rangle = \langle 0, u \rangle = 0,$$

159 the necessary condition for existence of a solution of (2.7) is $\langle 1, h \rangle = \int_{-\infty}^{\infty} h(y) dy = 0$.
 160 When this is satisfied, the solution is given by

$$161 \quad u(y) = -\Phi^Y(y) \int^y \frac{H(s)}{\Phi^Y(s)} ds + c\Phi^Y(y),$$

162 where the constant c is arbitrary (the second solution of the homogeneous equation
 163 is ruled out as noted above), and where $H(\cdot) = \int h(s) ds$ is an antiderivative of h .

164 **2.2. Outer region:** $t \gg O(\epsilon)$. Turning to the evolution of the transition density
 165 function, over timescales much longer than the mean reversion time ϵ , the volatility
 166 is effectively sampled from its ergodic distribution, as is already seen from (1.4), and
 167 will determine the first term of the asymptotic expansion.

168 We expand

$$169 \quad p^\epsilon(0, x_0, y_0; t, x, y) \sim p_0(t, x, y) + \sqrt{\epsilon}p_1(t, x, y) + \epsilon p_2(t, x, y) + \epsilon^{3/2}p_3(t, x, y) + \dots,$$

170 where here and henceforth we suppress the dependence on x_0 and y_0 unless it is
 171 needed.

172 Before proceeding, we note that, as p^ϵ is a probability density, $\iint_{\mathbb{R}^2} p^\epsilon dx dy = 1$
 173 for all t , and that similarly $\iint_{\mathbb{R}^2} p_0 dx dy = 1$ for all t (because of the initial condition),
 174 whereas $\iint_{\mathbb{R}^2} p_i dx dy = 0$ for $i > 0$. Moreover, the marginal densities

$$175 \quad p_{X_t}^\epsilon(t, x) = \int_{-\infty}^{\infty} p^\epsilon(t, x, y) dy, \quad p_{Y_t}^\epsilon(t, y) = \int_{-\infty}^{\infty} p^\epsilon(t, x, y) dx$$

176 each have their own expansions

$$177 \quad p_{X_t}^\epsilon(t, x) \sim p_{X_t,0} + \sqrt{\epsilon}p_{X_t,1} + \dots, \quad p_{Y_t}^\epsilon(t, y) \sim p_{Y_t,0} + \sqrt{\epsilon}p_{Y_t,1} + \dots,$$

178 and the first term in each expansion integrates in x (resp. in y) to 1 while the re-
 179 mainder integrate to zero, because each such integral is the double integral of a term
 180 in the original expansion of p^ϵ . Note, however, that it is possible for any truncated
 181 version of any of the expansions to fail to be a probability density by virtue of being
 182 negative somewhere; this is in practice invariably the case in the far tails of the dis-
 183 tributions where a separate (large-deviations/ray-theory) expansion would be needed
 184 to accurately capture the behaviour.

185 Now substituting into (2.1) and equating coefficients of powers of ϵ leads imme-
 186 diately to:

$$187 \quad (2.8) \quad \text{At } O(1/\epsilon): \quad -\mathcal{L}_0^* p_0 = 0;$$

$$188 \quad (2.9) \quad \text{At } O(1/\sqrt{\epsilon}): \quad -\mathcal{L}_0^* p_1 = \mathcal{L}_1^* p_0;$$

$$189 \quad (2.10) \quad \text{At } O(1): \quad -\mathcal{L}_0^* p_2 = -\partial_t p_0 + \mathcal{L}_2^* p_0 + \mathcal{L}_1^* p_1;$$

$$190 \quad (2.11) \quad \text{At } O(\sqrt{\epsilon}): \quad -\mathcal{L}_0^* p_3 = -\partial_t p_1 + \mathcal{L}_2^* p_1 + \mathcal{L}_1^* p_2;$$

192 the pattern in the last two of these repeats at still higher orders.

193 *Lowest order* $O(1/\epsilon)$. We have the leading order solution

$$194 \quad p_0(t, x, y) = f_0(t, x)\Phi^Y(y) + g_0(t, x)\Phi^Y(y) \int_{-\infty}^y \frac{ds}{\Phi^Y(s)},$$

195 where f_0 and g_0 are unknown at this stage; however, because p^ϵ is a probability
196 density, and must be integrable in both x and y , we have $g_0(t, x) = 0$, because the
197 function that it multiplies is not integrable. We shall see later that $\int_{-\infty}^{\infty} f_0(t, x) dx = 1$
198 and all other p_i then integrate to zero over \mathbb{R}^2 .

199 We note immediately that we cannot satisfy the initial condition (2.2); a separate
200 boundary-layer analysis, given in Subsection 2.3, is needed to resolve this.

201 At $O(1/\sqrt{\epsilon})$. From (2.9), we have

$$202 \quad (2.12) \quad -\mathcal{L}_0^* p_1 = \mathcal{L}_1^* p_0 = \rho_{xy} \nu \sqrt{2} (\partial_x f_0(t, x)) \partial_y (\sigma(y) \Phi^Y(y)).$$

204 As the y dependence on the right-hand side integrates to zero, this equation does have
205 an integrable solution, and it is

$$206 \quad (2.13) \quad p_1(t, x, y) = -\rho_{xy} \nu \sqrt{2} (\partial_x f_0(t, x)) \Sigma(y) \Phi^Y(y) + f_1(t, x) \Phi^Y(y),$$

207 where $\Sigma(y) = \int_{-\infty}^y \sigma(s) ds$ (if σ is not integrable at $-\infty$, we simply integrate from
208 (say) zero and amend $f_1(t, x)$ accordingly). Here $f_1(t, x)$ is again unknown; the other
209 solution of the homogeneous equation has been eliminated as above.

210 At $O(1)$. Now we have

$$\begin{aligned} 211 \quad -\mathcal{L}_0^* p_2 &= -\partial_t p_0 + \mathcal{L}_2^* p_0 + \mathcal{L}_1^* p_1 \\ 212 \quad &= -\Phi^Y(y) \left(\partial_t f_0(t, x) - \frac{1}{2} \sigma^2(y) \partial_{xx} f_0(t, x) + \partial_x (\mu(x, y) f_0(t, x)) \right) \\ 213 \quad &- 2\rho_{xy}^2 \nu^2 (\partial_{xx} f_0(t, x)) \partial_y (\sigma(y) \Sigma(y) \Phi^Y(y)) + \rho_{xy} \nu \sqrt{2} (\partial_x f_1(t, x)) \partial_y (\sigma(y) \Phi^Y(y)). \end{aligned}$$

215 The terms in the last line satisfy the solvability condition (as, indeed, does any func-
216 tion that is the result of applying \mathcal{L}_1^* to a function of y which vanishes at $\pm\infty$) and
217 so we need that the terms in the middle line integrate to zero. This leads directly to

$$218 \quad (2.14) \quad \partial_t f_0 = \frac{1}{2} \langle \sigma^2(\cdot) \rangle \partial_{xx} f_0 - \partial_x (\langle \mu(x, \cdot) \rangle f_0) = \langle \mathcal{L}_2^* \rangle f_0(t, x),$$

220 where we are introducing the notation $\langle \mathcal{L}_i^* \rangle$ for operators with coefficients averaged
221 over the ergodic distribution. Using this to eliminate $\partial_t f_0(t, x)$, we see that

$$222 \quad -\mathcal{L}_0^* p_2 = (\mathcal{L}_2^* - \langle \mathcal{L}_2^* \rangle) p_0 + \mathcal{L}_1^* p_1,$$

223 the solution of which consists of a particular solution plus a solution $f_2(t, x) \phi^Y(y)$ of
224 the inhomogeneous equation, $f_2(t, x)$ being as yet unknown.

225 As expected, $p_0(t, x, y)$ is the product of the ergodic density of Y and the density
226 of X with the stochastic parameters replaced with their means, so X and Y behave
227 independently at this order.

228 We need an initial condition for $f_0(t, x)$. Given the apparent independence of X
229 and Y at this order, we suspect that $f_0(t_0, x) = \delta(x - x_0)$, and this is confirmed by
230 the boundary-layer analysis of the next subsection.

231 At $O(\sqrt{\epsilon})$. Here we have

$$232 \quad -\mathcal{L}_0^* p_3 = -\partial_t p_1 + \mathcal{L}_2^* p_1 + \mathcal{L}_1^* p_2.$$

233 As noted above, the final term on the right-hand side automatically satisfies the solv-
234 ability condition and so we fix $f_1(t, x)$ by substituting for p_1 from (2.13), integrating
235 over y , and then solving

(2.15)

$$236 \quad \partial_t f_1 - \langle \mathcal{L}_2^* \rangle f_1 = \int_{-\infty}^{\infty} \left[\mathcal{L}_2^* \left(-\rho_{xy} \nu \sqrt{2} (\partial_x f_0(t, x)) \Sigma(y) \Phi^Y(y) \right) \right] dy$$

$$237 \quad = -\rho_{xy} \nu \sqrt{2} \left(\frac{1}{2} (\sigma^2(\cdot) \Sigma(\cdot)) \partial_{xx} (\partial_x f_0(t, x)) - \partial_x (\langle \mu(x, \cdot) \Sigma(\cdot) \rangle \partial_x f_0(t, x)) \right).$$

238

239 As $\Phi^Y(y)$ comes out as a factor, we have an ergodic average as before. The ini-
240 tial condition for this problem is found via the boundary-layer analysis of the next
241 subsection.

242 **2.3. Boundary layer near $t = 0$.** The analysis above fails when $t = O(\epsilon)$,
243 because there is an initial layer in which Y_t transits to its ergodic distribution. The
244 large-time limit of the boundary layer solution provides the initial conditions for the
245 functions $f_i(t, x)$ above, via asymptotic matching.

246 To capture this behaviour, we rescale time via

$$247 \quad t = \epsilon t'.$$

248 Then in the boundary layer the transition density, now denoted $p'(0, x_0, y_0; t', x, y)$,
249 satisfies

$$250 \quad (2.16) \quad \frac{1}{\epsilon} \partial_{t'} p' - \left(\frac{1}{\epsilon} \mathcal{L}_0^* + \frac{1}{\sqrt{\epsilon}} \mathcal{L}_1^* + \mathcal{L}_2^* \right) p' = 0,$$

251 with the initial condition

$$252 \quad (2.17) \quad p'(0, x_0, y_0; 0, x, y) = \delta(x - x_0) \otimes \delta(y - y_0).$$

253 We proceed exactly as above, expanding

$$254 \quad p'(0, x_0, y_0; t', x, y) \sim p'_0(t', x, y) + \sqrt{\epsilon} p'_1(t', x, y) + \epsilon p'_2(t', x, y) + \epsilon^{3/2} p'_3(t', x, y) + \dots,$$

255 and again suppressing the dependence on x_0 and y_0 unless it is needed. Substituting
256 into (2.16) and equating coefficients of powers of ϵ leads immediately to:

$$257 \quad (2.18) \quad \text{At } O(1/\epsilon): \quad (\partial_{t'} - \mathcal{L}_0^*) p'_0 = 0;$$

$$258 \quad (2.19) \quad \text{At } O(1/\sqrt{\epsilon}): \quad (\partial_{t'} - \mathcal{L}_0^*) p'_1 = \mathcal{L}_1^* p'_0;$$

$$259 \quad (2.20) \quad \text{At } O(1): \quad (\partial_{t'} - \mathcal{L}_0^*) p'_2 = \mathcal{L}_1^* p'_1 + \mathcal{L}_2^* p'_0;$$

$$260 \quad (2.21) \quad \text{At } O(\sqrt{\epsilon}): \quad (\partial_{t'} - \mathcal{L}_0^*) p'_3 = \mathcal{L}_1^* p'_2 + \mathcal{L}_2^* p'_1;$$

262 the pattern in the last two of these repeats at higher orders. The initial conditions
263 for the functions p'_i are

$$264 \quad p'_0(0, x, y) = \delta(x - x_0) \otimes \delta(y - y_0), \quad p'_i(0, x, y) = 0, \quad i = 1, 2, 3, \dots$$

At $O(1/\epsilon)$. We have the degenerate (because lacking in x -derivatives) parabolic equation

$$(\partial_{t'} - \mathcal{L}_0^*) p'_0 = 0, \quad p'_0(0, x, y) = \delta(x - x_0) \otimes \delta(y - y_0).$$

Now bearing in mind that for a Brownian motion W we have that $(1/\sqrt{\epsilon})W_t$ becomes a Brownian motion $W_{t'}$ under the time-change $t = \epsilon t'$, we have in law

$$dY_{t'} = \kappa(m - Y_{t'}) dt' + \nu\sqrt{2} dW_{t'},$$

the marginal density of this O-U process at time t' is Normal with mean and variance

$$m(t'; y_0) = m + (y_0 - m)e^{-\kappa t'}, \quad \text{var}(t') = \frac{\nu^2}{\kappa} \left(1 - e^{-2\kappa t'}\right),$$

respectively. It follows that

$$p'_0(t', x, y) = \delta(x - x_0) \phi^Y(t', y),$$

where

$$(2.22) \quad \phi^Y(t', y) = \frac{1}{\sqrt{2\pi \text{var}(t')}} e^{-(x - m(t'; y_0))^2 / 2\text{var}(t')}.$$

When necessary, this is interpreted in the sense of distributions. Note immediately that

$$\lim_{t' \rightarrow \infty} \phi^Y(t', y) = \Phi^Y(y)$$

as defined above. Hence the limit of $p_1(t', x, y)$ as $t' \rightarrow \infty$ is $\delta(x - x_0)\Phi(y)$ and (by asymptotic matching) this is the initial condition for $f_0(t, x)$,

$$(2.23) \quad f_0(t, x) = \delta(x - x_0).$$

The interpretation of this result is that, at leading order, X_t stays at its initial value x_0 while Y_t forgets its initial value and transits to its ergodic distribution. In fact, there is a small amount of diffusion of X_t , which is resolved by introducing a further (spatial) inner layer of size $O(\sqrt{\epsilon})$ around x_0 . With $x = x_0 + \sqrt{\epsilon}\xi$, $p'(t', x, y) = (1/\sqrt{\epsilon})P'(t', \xi, y)$, at leading order we have

$$(2.24) \quad \partial_{t'} P' - \left(\frac{1}{2} \sigma^2(y) \partial_{\xi\xi} + \rho_{xy} \nu \sqrt{2} \sigma(y) \partial_{\xi y} + \nu^2 \partial_{yy} \right) P' + \kappa \partial_y ((m - y) P') = 0,$$

$$(2.25) \quad P'(0, \xi, y) = \delta(\xi) \delta(y - y_0)$$

(note the appearance of the correlation term, brought in by a combination of its original coefficient of $1/\sqrt{\epsilon}$ and a further $1/\sqrt{\epsilon}$ from the change of variable to ξ). The solution of this equation (not, as far as we know, available in closed form) represents the slow (on the t' timescale) spreading out of the initial point mass of the marginal density of X , while Y transits to its ergodic distribution. We do not pursue this further.

At $O(1/\sqrt{\epsilon})$. The equation (2.19) for p'_1 now becomes

$$(2.26) \quad (\partial_{t'} - \mathcal{L}_0^*) p'_1 = \rho_{xy} \nu \sqrt{2} \delta'(x - x_0) \partial_y (\sigma(y) \phi^Y(t', y)).$$

As $t' \rightarrow \infty$, $\phi^Y(t', y) \rightarrow \Phi^Y(y)$ and hence the solution of this equation has the limiting time-independent form

$$(2.27) \quad -\rho_{xy} \nu \sqrt{2} \delta'(x - x_0) \Sigma(y) \Phi^Y(y) + c_1(x) \Phi^Y(y)$$

302 for some function $c_1(x)$ which provides the initial condition for $f_1(t, x)$, while the
 303 first term in (2.27) matches automatically with the corresponding part of the solution
 304 $p_1(t, x, y)$ as $t \downarrow 0$. Fortunately, we can find $c_1(x)$ without having to solve for p'_1
 305 (which we could do, using the Green's function which is, in effect, $\phi^Y(t', y)$). Inte-
 306 grating (2.26) over y , and noting that both \mathcal{L}_0^* and the right-hand side integrate to
 307 zero, we find

$$308 \quad \frac{d}{dt'} \int_{-\infty}^{\infty} p'_1(t', x, y) dy = 0$$

309 (this is essentially the orthogonality we used in the outer region) and hence the integral
 310 is equal to its initial value, namely zero. It follows that (2.27) must also integrate to
 311 zero. Bearing in mind that $\Phi^Y(y)$ is a probability density and so integrates to 1, we
 312 have

$$313 \quad c_1(x) = -\rho_{xy} \nu \sqrt{2} \delta'(x - x_0) \int_{-\infty}^{\infty} \Sigma(y) \Phi^Y(y) dy$$

$$314 \quad = -\rho_{xy} \nu \sqrt{2} \delta'(x - x_0) \langle \Sigma \rangle$$

$$315 \quad = f_1(0, x).$$

316 (2.28)

317 This is the initial condition for (2.15).

318 In summary, we have that $p_0(t, x, y) = f_0(t, x) \Phi^Y(y)$, where Φ^Y is given by (2.6)
 319 and f_0 solves (2.14) with initial datum (2.23); for μ which is constant in x , f_0 is simply
 320 a normal density. At $O(\sqrt{\epsilon})$, p_1 is given by (2.13) with f_1 satisfying (2.15) with initial
 321 condition (2.28). Note that $p_1(0, x, y) \neq 0$, confirming the need for the inner region.

322 **2.4. A global approximation and correction equation.** As we know the
 323 density of the O-U process Y to be $\Phi^Y(t/\epsilon, y)$, from (2.22), we can define an approx-
 324 imation globally in time as

$$325 \quad (2.29) \quad p_{0,\epsilon}(t, x, y) = \Phi^Y(t/\epsilon, y) f_0(t, x),$$

326 which has the correct initial datum $p_0^\epsilon(0, x, y) = \delta(x - x_0) \otimes \delta(y - y_0)$, the exact
 327 marginal density for Y_t , and is correct to leading order in ϵ in both the inner and
 328 outer layer. By insertion, we see directly that $p_{0,\epsilon}$ from (2.29) satisfies

$$329 \quad (2.30) \quad \partial_t p_{0,\epsilon} - \left(\frac{1}{\epsilon} \mathcal{L}_0^* + \langle \mathcal{L}_2^* \rangle \right) p_{0,\epsilon} = 0.$$

330

331 Taking the difference with (2.1), we have

$$332 \quad (2.31) \quad \partial_t (p^\epsilon - p_{0,\epsilon}) - \left(\frac{1}{\epsilon} \mathcal{L}_0^* + \frac{1}{\sqrt{\epsilon}} \mathcal{L}_1^* + \mathcal{L}_2^* \right) (p^\epsilon - p_{0,\epsilon}) = \frac{1}{\sqrt{\epsilon}} \mathcal{L}_1^* p_{0,\epsilon} + (\langle \mathcal{L}_2^* \rangle - \mathcal{L}_2^*) p_{0,\epsilon}.$$

333

334 Replacing the operator on the left-hand side in (2.31) by that in (2.30), we define a
 335 correction to p^ϵ by $p_{0,\epsilon} + p_{1,\epsilon}$, where

$$336 \quad (2.32) \quad \partial_t p_{1,\epsilon} - \left(\frac{1}{\epsilon} \mathcal{L}_0^* + \langle \mathcal{L}_2^* \rangle \right) p_{1,\epsilon} = \frac{1}{\sqrt{\epsilon}} \mathcal{L}_1^* p_{0,\epsilon} + (\langle \mathcal{L}_2^* \rangle - \mathcal{L}_2^*) p_{0,\epsilon}, \quad p_{1,\epsilon}(0, x, y) = 0.$$

337

338 This approach will be useful for the SPDE in the next section.

3. Perturbation analysis of the Zakai SPDE.

3.1. Set-up and preliminaries. The matched asymptotic expansion analysis for the KFE (1.2) shows the different ansatz needed for small times (the ‘inner layer’ in subsection 2.3), where the process Y transits from its initial value to the stationary distribution, and for all times after this initial transit (the ‘outer layer’ in 2.2). These two expressions can be reconciled by using the analytical exact form for the marginal law of Y and an expansion for the effect of Y on X only (see subsection 2.4).

For the SPDE (1.3), the presence of a fast driving process correlated to a slow driving process creates extra difficulties for a direct asymptotic expansion. In a formal expansion of the SPDE similar to that in Section 2 for the KFE, the appearance of $O(1/\sqrt{\epsilon})$ terms multiplying both W_t^y and the $\partial_x \partial_y$ terms makes it difficult to transfer the multiple scales expansion from the KFE to the Zakai SPDE. We note that [18] has to restrict the derivation of the limiting SPDE for $\epsilon \rightarrow 0$ (determining the zero order term) to the case $\rho = 0$.

To avoid this last issue and take advantage of a global approximation, we split Y into a component U which has the correct instantaneous correlation with X and a component Y^\dagger which is independent of X . We then study the joint dynamics of X and Y^\dagger conditional on (W^x, W^y) , keeping track of the dynamics of (U, Y^\dagger) and its law exactly, while we approximate the generator of X by an expansion.

Specifically, we introduce a process U as the (strong) solution to

$$(3.1) \quad dU_t = -\frac{\kappa}{\epsilon} U_t dt + \frac{\nu\sqrt{2}}{\sqrt{\epsilon}} \rho_y dW_t^y, \quad U_0 = 0.$$

Then $Y^\dagger := Y - U - m$ satisfies

$$(3.1) \quad dY_t^\dagger = -\frac{\kappa}{\epsilon} Y_t^\dagger dt + \frac{\nu\sqrt{2}}{\sqrt{\epsilon}} \sqrt{1 - \rho_y^2} dW_t^{y,1}, \quad Y_0^\dagger = y_0 - m,$$

where $W^{y,1}$ is independent of W^x and $W^{x,1}$, and W^x, W^y have correlation ρ . We set in the following $m = 0$ without loss of generality, as it simply results in a constant shift of the OU process; this can be accounted for in X by a horizontal translation of the function σ .

We will therefore study the two-dimensional Zakai SPDE for (X, Y^\dagger) , describing the marginal probability distribution of (X_t, Y_t^\dagger) conditional on the natural filtration $\mathcal{F}_t^{x,y}$ of $W = (W^x, W^y)$,

$$(3.2) \quad \begin{aligned} dv &= \frac{1}{\epsilon} \left(\nu^2 (1 - \rho_y^2) \partial_{yy} v + \kappa \partial_y (yv) \right) dt \\ &\quad + \left(\frac{1}{2} \sigma^2 (y + U_t) \partial_{xx} v - \mu \partial_x v \right) dt - \rho_x \sigma (y + U_t) \partial_x v dW_t^x \\ &= \left(\frac{1}{\epsilon} \tilde{\mathcal{L}}_0^* + \tilde{\mathcal{L}}_2^* \right) v dt - \rho_x \sigma (y + U_t) \partial_x v dW_t^x, \\ v(0, x, y) &= \delta(x - x_0) \otimes \delta(y - y_0), \end{aligned}$$

where, in analogy to earlier,

$$(3.2) \quad \tilde{\mathcal{L}}_0^* \cdot = \nu^2 (1 - \rho_y^2) \partial_{yy} \cdot - \kappa \partial_y (y \cdot), \quad \tilde{\mathcal{L}}_2^* \cdot = \frac{1}{2} \sigma^2 (y + U_t) \partial_{xx} \cdot - \mu \partial_x \cdot,$$

and where $\nu > 0$, $\kappa > 0$, $\rho_x \in (-1, 1)$, $0 < \epsilon \ll 1$ are fixed constants, $\sigma : \mathbb{R} \rightarrow \mathbb{R}_+$ is a real-valued function of which we will specify later any conditions needed. For simplicity, we consider $\mu \in \mathbb{R}$ a given constant.

375 We aim to find an expansion of the solution v to the SPDE (3.2) as $\epsilon \rightarrow 0$.

376 **3.2. Zero order term.** Following [18], and in line with the findings of Section
 377 2, we introduce the following SPDE akin (1.5), by averaging the coefficients over the
 378 stationary distribution,

$$\begin{aligned} 379 \quad (3.3) \quad dv_0^x &= \left(\frac{1}{2} \langle \sigma^2 \rangle \partial_{xx} v_0^x - \mu \partial_x v_0^x \right) dt - \rho_x \langle \sigma \rangle \partial_x v_0^x dW_t^x \\ &= \langle \tilde{\mathcal{L}}_2^* \rangle v_0^x dt - \rho_x \langle \sigma \rangle \partial_x v_0^x dW_t^X, \\ v_0^x(0, x) &= \delta(x - x_0), \end{aligned}$$

380 where $\langle \sigma \rangle$ and $\langle \sigma^2 \rangle$ are again the averages over the ergodic distribution and the
 381 operator $\langle \tilde{\mathcal{L}}_2^* \rangle$ is defined as

$$382 \quad (3.4) \quad \langle \tilde{\mathcal{L}}_2^* \rangle \cdot := \frac{1}{2} \langle \sigma^2 \rangle \partial_{xx} \cdot - \mu \partial_x \cdot .$$

383 The SPDE (3.3) has the analytic solution

$$\begin{aligned} 384 \quad (3.5) \quad v_0^x(t, x) &= \Psi(t, x) \\ 385 \quad (3.6) \quad &:= f_0(t, x - \rho_x \langle \sigma \rangle W_t^x) \\ 386 \quad &= \frac{1}{\sqrt{2\pi(\langle \sigma^2 \rangle - \rho_x^2 \langle \sigma \rangle^2)t}} \exp\left(-\frac{(x - x_0 - \mu t - \rho_x \langle \sigma \rangle W_t^x)^2}{2(\langle \sigma^2 \rangle - \rho_x^2 \langle \sigma \rangle^2)t}\right), \end{aligned}$$

387 where f_0 has been introduced earlier as solution to (2.14).

388 Now we include the initial transient of the processes Y^\dagger and U to their stationary
 389 distribution. The marginal density of the O-U process Y^\dagger at time t is known to be
 390 $\Phi^\dagger(t/\epsilon, y)$ with

$$391 \quad (3.7) \quad \Phi^\dagger(t', y) = \frac{1}{\sqrt{2\pi\sigma_\dagger^2(t')}} \exp\left(-\frac{(y - \mu_\dagger(t'))^2}{2\sigma_\dagger^2(t')}\right),$$

392 where $\mu_\dagger(t')$ and $\sigma_\dagger^2(t')$ have the form

$$393 \quad (3.8) \quad \mu_\dagger(t') = y_0 e^{-\kappa t'/\epsilon}, \quad \sigma_\dagger^2(t') = \frac{(1 - \rho_y^2)\nu^2}{\kappa} \left(1 - e^{-2\kappa t'/\epsilon}\right),$$

394 and it satisfies the PDE

$$\begin{aligned} 395 \quad \partial_t \Phi &= \frac{1}{\epsilon} \tilde{\mathcal{L}}_0^* \Phi = \frac{1}{\epsilon} (\nu^2(1 - \rho_y^2) \partial_{yy} \Phi + \kappa \partial_y (y\Phi)), \\ 396 \quad \Phi(0, y) &= \delta(y - y_0). \end{aligned}$$

398 Next, we follow the principle in Subsection 2.4 to define an approximation $v_{0,\epsilon}$
 399 for which we track U and keep the marginal density of Y^\dagger exact, but approximate the
 400 density of X given (Y^\dagger, U) , and hence the joint density. Therefore, we consider the
 401 equation

$$\begin{aligned} 402 \quad (3.9) \quad dv_{0,\epsilon} &= \frac{1}{\epsilon} (\nu^2(1 - \rho_y^2) \partial_{yy} v_{0,\epsilon} + \kappa \partial_y (y v_{0,\epsilon})) dt \\ &+ \left(\frac{1}{2} \langle \sigma^2 \rangle \partial_{xx} v_{0,\epsilon} - \partial_x (\mu v_{0,\epsilon}) \right) dt - \rho_x \langle \sigma \rangle \partial_x v_{0,\epsilon} dW_t^x \\ &= \left(\frac{1}{\epsilon} \tilde{\mathcal{L}}_0^* + \langle \tilde{\mathcal{L}}_2^* \rangle \right) v_{0,\epsilon} dt - \rho_x \langle \sigma \rangle \partial_x v_{0,\epsilon} dW_t^x. \end{aligned}$$

403 Moreover, equation (3.9) has the closed-form solution

$$404 \quad (3.10) \quad v_{0,\epsilon}(t, x, y) = \Psi(t, x) \Phi^\dagger(t/\epsilon, y),$$

405 where $\Psi(t, x)$ is defined in (3.5), and $\Phi^\dagger(t, y)$ is defined in (3.7). Note that $v_{0,\epsilon}$ satisfies
406 the correct initial condition

$$407 \quad v_{0,\epsilon}(0, x, y) = \delta(x - x_0) \otimes \delta(y - y_0).$$

408 We will later show numerically that $v_{0,\epsilon} - v \rightarrow 0$ in a weak sense as $\epsilon \rightarrow 0$.

409 **3.3. Correction terms.** The goal of this section is to construct successively
410 better approximations. We first derive an inhomogeneous SPDE for $v - v_{0,\epsilon}$. Taking
411 the difference between (3.2) and (3.9), we obtain
(3.11)

$$\begin{aligned} d(v - v_{0,\epsilon}) &= \left(\frac{1}{\epsilon} \tilde{\mathcal{L}}_0^* + \tilde{\mathcal{L}}_2^* \right) (v - v_{0,\epsilon}) dt - \rho_x \sigma(y + U_t) \partial_x (v - v_{0,\epsilon}) dW_t^x \\ &\quad - \frac{1}{2} \left(\langle \sigma^2 \rangle - \sigma^2(y + U_t) \right) \partial_{xx} v_{0,\epsilon} dt + \rho_x (\langle \sigma \rangle - \sigma(y + U_t)) \partial_x v_{0,\epsilon} dW_t^x, \\ (v - v_{0,\epsilon})(0, x, y) &= 0. \end{aligned}$$

413 Intuitively, the effect of the terms in the second line in (3.11) is expected to be small
414 for small ϵ , as the fast process U averages the terms involving $\sigma(\cdot + U_t)$ and $\sigma^2(\cdot + U_t)$
415 over the stationary distribution of U , while the presence of the dominant term $\tilde{\mathcal{L}}_0^*$
416 on the left-hand side effects an additional averaging over the stationary distribution
417 of Y^\dagger ; the combined effect is an averaging over the stationary distribution of Y over
418 timescales of order 1, so that the right-hand side, and hence the solution $v - v_{0,\epsilon}$, will
419 be small.

420 Similar to before, we define $v_{1,\epsilon}$ as the leading order approximation to $v - v_{0,\epsilon}$,
(3.12)

$$\begin{aligned} dv_{1,\epsilon} &= \left(\frac{1}{\epsilon} \tilde{\mathcal{L}}_0^* + \langle \tilde{\mathcal{L}}_2^* \rangle \right) v_{1,\epsilon} dt - \rho_x \langle \sigma \rangle \partial_x v_{1,\epsilon} dW_t^x \\ &\quad - \frac{1}{2} \left(\langle \sigma^2 \rangle - \sigma^2(y + U_t) \right) \partial_{xx} v_{0,\epsilon} dt + \rho_x (\langle \sigma \rangle - \sigma(y + U_t)) \partial_x v_{0,\epsilon} dW_t^x, \\ v_{1,\epsilon}(0, x, y) &= 0. \end{aligned}$$

422 In this definition, coming from (3.11), which describes the exact error, we have ap-
423 proximated \mathcal{L}_2^* by $\langle \tilde{\mathcal{L}}_2^* \rangle$ and σ by $\langle \sigma \rangle$ in the first line.

424 Given $v_{0,\epsilon}$ in (3.9), and $v_{1,\epsilon}$ in (3.12), we can recursively find higher order correc-
425 tions as follows:

$$\begin{aligned} (3.13) \quad dv_{n+1,\epsilon} &= \left(\frac{1}{\epsilon} \tilde{\mathcal{L}}_0^* + \langle \tilde{\mathcal{L}}_2^* \rangle \right) v_{n+1,\epsilon} dt - \rho_x \langle \sigma \rangle \partial_x v_{n+1,\epsilon} dW_t^x \\ &\quad - \frac{1}{2} \left(\langle \sigma^2 \rangle - \sigma^2(y + U_t) \right) \partial_{xx} v_{n,\epsilon} dt + \rho_x (\langle \sigma \rangle - \sigma(y + U_t)) \partial_x v_{n,\epsilon} dW_t^x, \\ v_{n+1,\epsilon}(0, x, y) &= 0. \end{aligned}$$

427 **3.4. Approximation to the marginal density of X .** One would hope that
428 the expansion in subsection 3.3 allows a computationally more efficient approximation
429 to the solution than solving the original two-dimensional SPDE directly numerically.

430 This is not clear when considering (3.12) directly, as the solution still depends on
431 x and y . If we were to drop $\tilde{\mathcal{L}}_0^*$ in (3.12), justified after the initial transient, the SPDE

432 is parametrised by y , so essentially two-dimensional if the solution for all x and y is
 433 needed.

434 However, in practical applications (see, e.g., Section 5), one is often only interested
 435 in the marginal law of X , characterised by the marginal density

$$436 \quad v^x(t, x) = \int_{-\infty}^{\infty} v(t, x, y) \, dy.$$

437 Integrating (3.9) over y gives the zero order approximation

$$438 \quad v_0^x = \int_{-\infty}^{\infty} v_{0,\epsilon}(t, x, y) \, dy = \Psi(t, x),$$

439 where $\Psi(t, x)$ is given by (3.5).

440 As for the first order term $v_{1,\epsilon}$, we similarly define v_1^x as

$$441 \quad v_1^x = \int_{-\infty}^{\infty} v_{1,\epsilon}(t, x, y) \, dy.$$

442 If we assume $\lim_{y \rightarrow \pm\infty} v_{1,\epsilon}(t, x, y) = 0$, $\lim_{y \rightarrow \pm\infty} \partial_y v_{1,\epsilon}(t, x, y) = 0$, it follows that

$$443 \quad \int_{-\infty}^{\infty} \tilde{\mathcal{L}}_0^* v_{1,\epsilon} \, dy = 0.$$

444 Moreover, from (3.10) and (3.7),

$$\begin{aligned} (3.14) \quad \int_{-\infty}^{\infty} \sigma^2(y + U_t) \partial_{xx} v_{0,\epsilon}(t, x, y) \, dy &= \int_{-\infty}^{\infty} \sigma^2(y + U_t) \partial_{xx} \Psi(t, x) \Phi^\dagger(t, y) \, dy \\ &= \partial_{xx} \Psi(t, x) \int_{-\infty}^{\infty} \sigma^2(y + U_t) \Phi_\infty^\dagger(y) \, dy + o(\epsilon^r) \\ 445 \quad &= \langle \sigma^2(\cdot + U_t) \rangle_\dagger \partial_{xx} \Psi(t, x) + o(\epsilon^r), \quad \forall r > 0, \\ \int_{-\infty}^{\infty} \sigma(y + U_t) \partial_x v_{0,\epsilon}(t, x, y) \, dy &= \int_{-\infty}^{\infty} \sigma(y + U_t) \partial_x \Psi(t, x) \Phi_\infty^\dagger(y) \, dy + o(\epsilon^r) \\ &= \langle \sigma(\cdot + U_t) \rangle_\dagger \partial_x \Psi(t, x) + o(\epsilon^r), \quad \forall r > 0, \end{aligned}$$

446 for fixed $t > 0$, and where $\Phi_\infty^\dagger = \lim_{t \rightarrow \infty} \Phi^\dagger(t/\epsilon, \cdot) = \lim_{\epsilon \rightarrow 0} \Phi^\dagger(t/\epsilon, \cdot)$, the stationary
 447 density of Y^\dagger , $\langle \cdot \rangle_\dagger$ the average over that distribution, and noting from (3.7), (3.8) that
 448 convergence of $\Phi^\dagger(t/\epsilon, \cdot)$ to Φ_∞^\dagger is exponential in ϵ .

449 Integrating (3.12) over y yields an SPDE for a first order approximation $v_{1,\epsilon}^x(t, x)$
 450 to $v^x(t, x)$,

$$\begin{aligned} dv_{1,\epsilon}^x &= \langle \tilde{\mathcal{L}}_2^* \rangle v_{1,\epsilon}^x \, dt - \rho_x \langle \sigma \rangle \partial_x v_{1,\epsilon}^x \, dW_t^x \\ &\quad - \frac{1}{2} (\langle \sigma^2 \rangle - \langle \sigma^2(\cdot + U_t) \rangle_\dagger) \partial_{xx} \Psi(t, x) \, dt \\ 451 \quad (3.15) \quad &\quad + \rho_x (\langle \sigma \rangle - \langle \sigma(\cdot + U_t) \rangle_\dagger) \partial_x \Psi(t, x) \, dW_t^x, \\ v_{1,\epsilon}^x(0, x) &= 0. \end{aligned}$$

452 **4. Numerical schemes for the Zakai SPDEs.** In this section, we present
 453 numerical schemes for the SPDEs introduced in the previous section. We will use
 454 these in Section 5 to test the accuracy of the expansion solutions.

455 The most challenging equation among those considered is the original SPDE (3.2),
 456 repeated here for convenience,

$$\begin{aligned}
 457 \quad & dv = \frac{1}{\epsilon} \left(\nu^2 (1 - \rho_y^2) \partial_{yy} v + \kappa \partial_y (yv) \right) dt \\
 458 \quad (4.1) \quad & + \left(\frac{1}{2} \sigma^2 (y + U_t) \partial_{xx} v - \mu \partial_x v \right) dt - \rho_x \sigma (y + U_t) \partial_x v dW_t^x, \\
 459 \quad & v(0, x, y) = \delta(x - x_0) \otimes \delta(y - y_0),
 \end{aligned}$$

$$\begin{aligned}
 460 \quad (4.2) \quad & dU_t = -\frac{\kappa}{\epsilon} U_t dt + \frac{\nu\sqrt{2}}{\sqrt{\epsilon}} \rho_y dW_t^y, \quad U_0 = 0. \\
 461
 \end{aligned}$$

462 A principal difficulty in solving this two-dimensional SPDE arises from the fact that
 463 we seek numerical solutions which are stable and accurate uniformly across all ϵ .

464 We will also be solving the SPDE (3.11) to determine the error of the zero-order
 465 approximation, and the SPDE (3.12) for the first order correction, by straightforward
 466 modifications of the scheme for (3.2).

467 The zero-order marginal approximation in x , v_0^x , is given in analytic form by
 468 Ψ in (3.5), while the correction term $v_{1,\epsilon}^x$ is given by (3.15) and can be found by a
 469 one-dimensional SPDE scheme.

470 We apply a Milstein ADI scheme to the SPDE (4.1), and an Euler scheme to the
 471 SDE (4.2), taking care to maintain uniform stability and accuracy for small ϵ . We
 472 achieve this by a semi-implicit approximation of the Zakai SPDE and an approxima-
 473 tion of the SDEs on a time mesh that scales with ϵ , as detailed below.

474 **4.1. Simulation of the OU-process.** We simulate the Ornstein–Uhlenbeck
 475 process (4.2) with timestep $k\epsilon$. It was found empirically in [6] that the simulated
 476 process using the Euler–Maruyama scheme then has a strong error independent of
 477 ϵ . This does not change the total computational effort significantly since the cost of
 478 simulating U is typically much smaller than solving the SPDE for v .

479 The discrete-time approximation of (U_t) is thus generated by

$$\begin{aligned}
 480 \quad (4.3) \quad & \widehat{U}_n = \widehat{U}_{n-1} - \kappa k \widehat{U}_{n-1} + \nu\sqrt{2}\rho_y \left(W_{t_n}^y - W_{t_{n-1}}^y \right), \\
 & \widehat{U}_0 = 0,
 \end{aligned}$$

481 where $n = 1, 2, \dots, t_n - t_{n-1} = k\epsilon$.

482 In practice, we first generate the bivariate standard normal random variables
 483 $(Z_{n,x}, Z_{n,y})$ with correlation ρ , where $n = 1, 2, \dots, NN_\epsilon$, $N_\epsilon = 1/\epsilon$, and where we
 484 assume for simplicity $1/\epsilon \in \mathbb{Z}$. We generate

$$485 \quad \widehat{U}_n = \widehat{U}_{n-1} - \frac{\kappa}{\epsilon} k \widehat{U}_{n-1} + \frac{\nu\sqrt{2}}{\sqrt{\epsilon}} \rho_y \sqrt{k} \left(Z_{n,y} - Z_{n-1,y} \right),$$

486 where $\widehat{U}_0 = 0$ and $n = 1, 2, \dots, NN_\epsilon$. Then we take

$$487 \quad (4.4) \quad U^n = \widehat{U}_{nN_\epsilon}, \quad n = 1, 2, \dots, N,$$

488 as the approximation to the process U_t at time $t = nk$, i.e., at the n -th time step on
 489 the coarser time mesh with width k , on which we will approximate the SPDE.

490 The Brownian increment of W^x over a “large” timestep k is thus

$$491 \quad W_{nk}^x - W_{(n-1)k}^x = \sqrt{k} \widetilde{Z}_{n,x} := \sum_{i=1}^{N_\epsilon} \sqrt{k\epsilon} Z_{N_\epsilon(n-1)+i,x},$$

492 which has the correct correlation ρ with W^y . Hence, we get

$$493 \quad \tilde{Z}_{n,x} = \sqrt{\epsilon} \sum_{i=1}^{N_\epsilon} Z_{N_\epsilon(n-1)+i,x}.$$

494 To simplify the notation, we write $Z_{n,x}$ instead of $\tilde{Z}_{n,x}$ in the following.

495 **4.2. Approximation of the one-dimensional SPDE.** The scheme we use for
496 the marginal SPDE for $v_{1,\epsilon}^x(t,x)$ from (3.15) is an adaptation of the schemes proposed
497 in [23, 24]. We consider a mesh $\mathcal{X} = (x_i)_{-I \leq i < I}$ for some integer I , $h_x > 0$ given, and
498 define an approximation $V_{i,1,x}^n$ to $v_{1,\epsilon}^x(t_n, x_i)$ by

$$(4.5) \quad \begin{aligned} & \left(I - \frac{\langle \sigma^2 \rangle}{2} \frac{k}{h_x^2} D_{xx} + \mu \frac{k}{2h_x} D_x \right) V_{1,x}^{n+1} \\ &= \left(I - \rho_x \langle \sigma \rangle \frac{\sqrt{k} Z_{n,x}}{2h_x} D_x + \rho_x^2 \langle \sigma \rangle^2 \frac{k(Z_{n,x}^2 - 1)}{2h_x^2} D_{xx} \right) V_{1,x}^n \\ & \quad - \frac{1}{2} \left(\langle \sigma^2 \rangle - \langle \sigma^2(\cdot + U^n) \rangle_{\dagger} \right) k \Psi_{xx}(nk, \mathcal{X}) + \rho_x \left(\langle \sigma \rangle - \langle \sigma(\cdot + U^n) \rangle_{\dagger} \right) \Psi_x(nk, \mathcal{X}) \sqrt{k} Z_{n,x} \\ & \quad + \frac{1}{2} \rho_x^2 \left(\langle \sigma \rangle - \langle \sigma(\cdot + U_i) \rangle_{\dagger} \right)^2 \Psi_{xx}(nk, \mathcal{X}) k(Z_{n,x}^2 - 1), \end{aligned}$$

500 where the operators D_x and D_{xx} are defined as the standard finite difference matrices
501 with

$$502 \quad (D_x V)_i = V_{i+1} - V_{i-1}, \quad (D_{xx} V)_i = V_{i+1} - 2V_i + V_{i-1},$$

504 U^n is found from (4.4), and where $\Psi_x(nk, \mathcal{X})$ and $\Psi_{xx}(nk, \mathcal{X})$ are the value of the
505 functions applied on the mesh X , i.e., $\Psi_x(nk, \mathcal{X})$ is the vector of values $\Psi_x(nk, x_i)$,
506 with Ψ from (3.5).

507 The scheme is semi-implicit to ensure stability in L_2 irrespective of the step
508 sizes. The terms in the first line of (4.5) hence come from an implicit finite difference
509 discretisation of the operator $\langle \mathcal{L}_2^* \rangle$; the second line contains an Euler–Maruyama term
510 for the Brownian integral, and the Milstein correction for strong first order in k ; the
511 last two lines use the exact expressions of Ψ and its derivatives in the inhomogeneous
512 terms and a Milstein approximation to the Brownian integral.

513 4.3. Approximation of the two-dimensional SPDEs.

514 **Original SPDE.** We approximate the SPDE (3.2) with an alternating direction
515 implicit (ADI) scheme of the operators $\tilde{\mathcal{L}}_0^*$ and $\tilde{\mathcal{L}}_2^*$, and a Milstein approximation of
516 the Brownian integral.

517 We use a spatial mesh with uniform spacing $h_x, h_y > 0$, and, for $T > 0$ fixed,
518 N time steps of size $k = T/N$. Let $V_{i,j}^n$ be the approximation to $v(nk, ih_x, jh_y)$,
519 $n = 1, \dots, N$, $i, j \in \mathbb{Z}$.

520 Adapting the schemes from [25] to our setting,

$$(4.6) \quad \begin{aligned} & \left(I - \frac{\nu^2(1 - \rho_y^2)}{\epsilon} \frac{k}{h_y^2} D_{yy} - \frac{\kappa}{\epsilon} \frac{k}{2h_y} D_y \mathcal{Y} \right) \left(I - \frac{\sigma^2(\mathcal{Y} + U^{n+1})}{2} \frac{k}{h_x^2} D_{xx} + \mu \frac{k}{2h_x} D_x \right) V^{n+1} \\ &= \left(I - \rho_x \sigma(\mathcal{Y} + U^n) \frac{\sqrt{k} Z_{n,x}}{2h_x} D_x + \rho_x^2 \sigma^2(\mathcal{Y} + U^n) \frac{k(Z_{n,x}^2 - 1)}{2h_x^2} D_{xx} \right) V^n, \end{aligned}$$

522 where U^n is from (4.4), and D_x, D_y standard finite difference matrices defined by

$$\begin{aligned}
523 \quad (D_x V)_{i,j} &= V_{i+1,j} - V_{i-1,j}, & (D_y V)_{i,j} &= V_{i,j+1} - V_{i,j-1}, \\
524 \quad (D_{xx} V)_{i,j} &= V_{i+1,j} - 2V_{i,j} + V_{i-1,j}, & (D_{yy} V)_{i,j} &= V_{i,j+1} - 2V_{i,j} + V_{i,j-1}, \\
525 \quad (D_{xy} V)_{i,j} &= V_{i+1,j+1} - V_{i-1,j+1} - V_{i+1,j-1} + V_{i-1,j-1}.
\end{aligned}$$

527 Moreover, \mathcal{Y} is the diagonal matrix such that each element of the diagonal corresponds
528 to a mesh point $(x_i, y_j) = (ih_x, jh_y)$, ordered the same way as V , so that for instance,
529 by slight abuse of notation, $\sigma(\mathcal{Y} + U^n)$ is a diagonal matrix where the entry corre-
530 sponding to point (ih_x, jh_y) is $(\sigma(\mathcal{Y} + U^n))_{i,j} = \sigma(y_j + U^n)$. V^0 is an approximation
531 of the initial condition to the SPDE (3.2).

532 The implicit treatment of $\tilde{\mathcal{L}}_2^*$ and particularly $\tilde{\mathcal{L}}_0^*$ is important for stability for all
533 mesh parameters and especially for all ϵ , as demonstrated by Proposition 4.1 below.
534 The ADI factorisation allows an efficient solution of the implicit scheme by a sequence
535 of tridiagonal systems.

536 PROPOSITION 4.1. *Provided that*

$$537 \quad (4.7) \quad |\rho_x| \leq \frac{1}{\sqrt[4]{2}} \frac{\inf_{y \in \mathbb{R}} \sigma(y)}{\sup_{y \in \mathbb{R}} \sigma(y)},$$

538 the scheme (4.6) is stable in the ℓ_2 -norm, $|V|_2^2 := \sum_{i,j} V_{i,j}^2$. Specifically, for all $\epsilon > 0$,
539 $h_x, h_y > 0$ and k, N with $kN = T$, $k\epsilon y_{\max}^2 \leq \nu^2(1 - \rho_y^2)$, we have

$$540 \quad (4.8) \quad \mathbb{E}|V^n|_2^2 \leq \exp\left(\frac{T\epsilon y_{\max}^2}{\nu^2(1 - \rho_y^2)}\right) |V^0|_2^2.$$

541 *Proof.* We consider the discrete-continuous Fourier pair

$$542 \quad V_{l,j}^n = \int_{-\pi}^{\pi} \tilde{V}_j^n(\omega) e^{i\omega l} d\omega, \quad \tilde{V}_j^n(\omega) = \frac{1}{2\pi} \sum_{l=-\infty}^{\infty} V_{l,j}^n e^{-i\omega l}.$$

543 By insertion and standard algebraic manipulations,

$$544 \quad (4.9) \quad \left((I - kL_y) \tilde{V}^{n+1}(\omega) \right)_j = \frac{\tilde{L}_{x,j}^{\text{ex},n}}{\tilde{L}_{x,j}^{\text{im},n}} \tilde{V}_j^n(\omega),$$

545 where

$$\begin{aligned}
547 \quad (L_y \tilde{V}^n)_j &= \frac{\nu^2(1 - \rho_y^2)}{\epsilon} \frac{1}{h_y^2} \left(\tilde{V}_{j+1}^n - 2\tilde{V}_j^n + \tilde{V}_{j-1}^n \right) - \frac{\kappa}{\epsilon} \frac{1}{2h_y} \left(y_{j+1} \tilde{V}_{j+1}^n - y_{j-1} \tilde{V}_{j-1}^n \right) \\
548 \quad \tilde{L}_{x,j}^{\text{ex},n} &= 1 - i\rho_x \sigma(y_j + U^n) \frac{\sqrt{k}}{h_x} \sin(\omega) Z_n - 2\rho_x^2 \frac{k}{h_x^2} \sin^2(\omega/2) (Z_n^2 - 1), \\
549 \quad \tilde{L}_{x,j}^{\text{im},n} &= 1 + 2\sigma^2(y_j + U^{n+1}) \frac{k}{h_x^2} \sin^2(\omega/2) + i \frac{k}{h_x} \sin(\omega).
\end{aligned}$$

551 Multiplying the left-hand side of (4.9) by $\tilde{V}_j^{n+1,*}$, with $*$ denoting the complex con-
552 jugate, summing over j and carrying out summation by parts,

$$553 \quad - \sum_j (L_y \tilde{V}^{n+1})_j \tilde{V}_j^{n+1,*} = \frac{\nu^2(1 - \rho_y^2)}{\epsilon} \frac{|\tilde{V}_{j+1}^{n+1} - \tilde{V}_j^{n+1}|^2}{h_y^2} + \frac{\kappa}{\epsilon} y_j \tilde{V}_j^{n+1} \frac{(\tilde{V}_{j+1}^{n+1} - \tilde{V}_{j-1}^{n+1})^*}{2h_y}.$$

554

555 Writing in the last term $\tilde{V}_{j+1}^{n+1} - \tilde{V}_{j-1}^{n+1} = (\tilde{V}_{j+1}^{n+1} - \tilde{V}_j^{n+1}) + (\tilde{V}_j^{n+1} - \tilde{V}_{j-1}^{n+1})$, shifting
556 the index in the summation, apply Young's inequality as

$$557 \quad \frac{1}{2}(y_j \tilde{V}_j^{n+1} + y_{j+1} \tilde{V}_{j+1}^{n+1}) \frac{(\tilde{V}_{j+1}^{n+1} - \tilde{V}_j^{n+1})^*}{h_y} \geq$$

$$558 \quad - \frac{\nu^2(1 - \rho_y^2)}{\epsilon} \frac{|\tilde{V}_{j+1}^{n+1} - \tilde{V}_j^{n+1}|^2}{h_y^2} - \frac{\epsilon |y_j \tilde{V}_j^{n+1} + y_{j+1} \tilde{V}_{j+1}^{n+1}|^2}{8\nu^2(1 - \rho_y^2)}.$$

560 Upon a further application of Young's inequality and insertion,

$$561 \quad \sum_j \left((I - kL_y) \tilde{V}^{n+1} \right)_j \tilde{V}_j^{n+1,*} \geq \sum_j |\tilde{V}_j^{n+1}|^2 - k \sum_j \frac{\epsilon |y_j \tilde{V}_j^{n+1}|^2}{2\nu^2(1 - \rho_y^2)}$$

$$562 \quad (4.10) \quad \geq \left(1 - k \frac{\epsilon y_{\max}^2}{2\nu^2(1 - \rho_y^2)} \right) \sum_j |\tilde{V}_j^{n+1}|^2.$$

564 To estimate the right-hand side of (4.9),

$$565 \quad \mathbb{E}[|\tilde{L}_{x,j}^{\text{ex},n}|^2 | \mathcal{F}_{t_n}] = 1 + \rho_x^2 \sigma^2(y_j + U^n) \frac{k}{h_x^2} \sin^2(\omega) + 8\rho_x^4 \frac{k^2}{h_x^4} \sin^4(\omega/2)$$

$$566 \quad \leq \left(1 + 2\sqrt{2} \sup_{y \in \mathbb{R}} \sigma^2(y) \frac{k}{h_x^2} \sin^2(\omega/2) \right)^2,$$

$$567 \quad |\tilde{L}_{x,j}^{\text{im},n}|^2 \geq \left(1 + 2 \inf_{y \in \mathbb{R}} \sigma^2(y) \frac{k}{h_x^2} \sin^2(\omega/2) \right)^2.$$

569 Hence, assuming (4.7),

$$570 \quad \mathbb{E} \left[\frac{|\tilde{L}_{x,j}^{\text{ex},n}|^2}{|\tilde{L}_{x,j}^{\text{im},n}|^2} \middle| \mathcal{F}_{t_n} \right] \leq 1.$$

572 On the right-hand side of (4.9), we have

$$573 \quad (4.11) \quad \sum_j \frac{\tilde{L}_{x,j}^{\text{ex},n}}{\tilde{L}_{x,j}^{\text{im},n}} \tilde{V}_j^n \tilde{V}_j^{n+1,*} \leq \frac{1}{2} \sum_j \left| \frac{\tilde{L}_{x,j}^{\text{ex},n}}{\tilde{L}_{x,j}^{\text{im},n}} \right|^2 |\tilde{V}_j^n|^2 + \frac{1}{2} \sum_j |\tilde{V}_j^{n+1}|^2.$$

575 From (4.9), (4.10) and (4.11),

$$576 \quad \left(1 - k \frac{\epsilon y_{\max}^2}{2\nu^2(1 - \rho_y^2)} \right) \sum_j \mathbb{E}[|\tilde{V}_j^{n+1}|^2 | \mathcal{F}_{t_n}] \leq \frac{1}{2} \sum_j |\tilde{V}_j^n|^2 + \frac{1}{2} \sum_j \mathbb{E}[|\tilde{V}_j^{n+1}|^2 | \mathcal{F}_{t_n}].$$

577 Rearranging, using Parseval's identity, and $1 - \delta/2 \geq \exp(-\delta)$ for any $0 \leq \delta \leq 1$,
578 we obtain (4.8) by induction over n . \square

579 The proof of Proposition 4.1 is more complicated than similar results in the lit-
580 erature, in that

- 581 • we seek stability with a constant independent of ϵ ,
- 582 • the coefficients depend on the fast process Y , and
- 583 • the coefficients are variable in y .

584 We address this by a combination of a Fourier transform in x to take advantage of
 585 the constant coefficients as in a standard von Neumann stability analysis, and an
 586 energy-type argument for the y direction as is common in the finite element and finite
 587 difference literature.

588 *Remark 4.2.* Note that (4.7) could be replaced by the simpler condition $\sqrt{2}\rho_x^2 \leq 1$
 589 if the term $\sigma^2(\mathcal{Y} + U^{n+1})$ on the left-hand side of (4.6) was replaced by $\sigma^2(\mathcal{Y} + U^n)$.
 590 The need to use the crude bounds on σ comes from the fact that we cannot control
 591 the difference between U^{n+1} and U^n , especially for small ϵ .

592 **Zero-order approximation (in ϵ).** For the zero order term $v_{0,\epsilon}$, we denote the
 593 corresponding numerical solution as V_0 , with the scheme
 (4.12)

$$\begin{aligned} & \left(I - \frac{\nu^2(1 - \rho_y^2)}{\epsilon} \frac{k}{h_y^2} D_{yy} - \frac{\kappa}{\epsilon} \frac{k}{2h_y} D_y \mathcal{Y} \right) \left(I - \frac{\langle \sigma^2 \rangle}{2} \frac{k}{h_x^2} D_{xx} + \mu \frac{k}{2h_x} D_x \right) V_0^{n+1} \\ 594 & = \left(I - \rho_x \langle \sigma \rangle \frac{\sqrt{k} Z_{n,x}}{2h_x} D_x + \rho_x^2 \langle \sigma \rangle^2 \frac{k(Z_{n,x}^2 - 1)}{2h_x^2} D_{xx} \right) V_0^n, \end{aligned}$$

595 with notation as earlier. Note that the closed-form solution to V_0 is (3.10), and
 596 $\langle \sigma \rangle$, $\langle \sigma^2 \rangle$ will be computed analytically for specific choices of $\sigma(\cdot)$ in the next section.

597 To determine the error (in ϵ) of the zero-order approximation, we can directly
 598 solve the SPDE for $v - v_{0,\epsilon}$ from (3.11). Denoting the solution as \tilde{V}_0 , we have the
 599 scheme

$$\begin{aligned} & \left(I - \frac{\nu^2(1 - \rho_y^2)}{\epsilon} \frac{k}{h_y^2} D_{yy} - \frac{\kappa}{\epsilon} \frac{k}{2h_y} D_y \mathcal{Y} \right) \left(I - \frac{\sigma^2(\mathcal{Y} + U^{n+1})}{2} \frac{k}{h_x^2} D_{xx} + \mu \frac{k}{2h_x} D_x \right) \tilde{V}_0^{n+1} \\ 600 & = \left(I - \rho_x \sigma(\mathcal{Y} + U^n) \frac{\sqrt{k} Z_{n,x}}{2h_x} D_x + \rho_x^2 \sigma^2(\mathcal{Y} + U^n) \frac{k(Z_{n,x}^2 - 1)}{2h_x^2} D_{xx} \right) \tilde{V}_0^{n+1} \\ & \quad - \frac{1}{2} \left(\langle \sigma^2 \rangle - \sigma^2(\mathcal{Y} + U_t) \right) k(\partial_{xx} V_0^n) + \rho_x \left(\langle \sigma \rangle - \sigma(\mathcal{Y} + U_t) \right) (\partial_x V_0^n) \sqrt{k} Z_{n,x} \\ & \quad + \frac{1}{2} \rho_x^2 \left(\langle \sigma \rangle - \sigma(\mathcal{Y} + U_t) \right)^2 (\partial_{xx} V_0^n) k(Z_{n,x}^2 - 1), \end{aligned}$$

601 where we use the analytic solution (3.10) to compute $\partial_x V_0^n = (\partial_x v_{0,\epsilon}(t_n, x_i, y_j))_{i,j}$,
 602 and similarly for $\partial_{xx} V_0$, and the initial condition $\tilde{V}_0^0 = 0$.

603 **First-order correction (in ϵ).** Similarly, the scheme for the approximation of
 604 the first-order term (3.12), denoted by V_1 , is

$$\begin{aligned} & \left(I - \frac{\nu^2(1 - \rho_y^2)}{\epsilon} \frac{k}{h_y^2} D_{yy} - \frac{\kappa}{\epsilon} \frac{k}{2h_y} D_y \mathcal{Y} \right) \left(I - \frac{\langle \sigma^2 \rangle}{2} \frac{k}{h_x^2} D_{xx} + \mu \frac{k}{2h_x} D_x \right) V_1^{n+1} \\ 605 & = \left(I - \rho_x \langle \sigma \rangle \frac{\sqrt{k} Z_{n,x}}{2h_x} D_x + \rho_x^2 \langle \sigma \rangle^2 \frac{k(Z_{n,x}^2 - 1)}{2h_x^2} D_{xx} \right) V_1^n \\ & \quad - \frac{1}{2} \left(\langle \sigma^2 \rangle - \sigma^2(\mathcal{Y} + U_t) \right) k(\partial_{xx} V_0^n) + \rho_x \left(\langle \sigma \rangle - \sigma(\mathcal{Y} + U_t) \right) (\partial_x V_0^n) \sqrt{k} Z_{n,x} \\ & \quad + \frac{1}{2} \rho_x^2 \left(\langle \sigma \rangle - \sigma(\mathcal{Y} + U_t) \right)^2 (\partial_{xx} V_0^n) k(Z_{n,x}^2 - 1), \end{aligned}$$

606 with zero initial condition, $V_1^0 = 0$. We also use the analytic solution for $\partial_x V_0$ and
 607 $\partial_{xx} V_0$ in the scheme (4.14).

608 In the computations below, we make some further specifications.

609 **5. Numerical results.** In this section, we illustrate the convergence of the ex-
 610 pansion for the model (3.2) by way of numerical tests. For illustration, we use the
 611 following Gaussian distribution as initial condition:

$$612 \quad (5.1) \quad v(0, x, y) = \Psi(t_0, x; W_{t_0}^x = 0) \Phi^\dagger(t_0, y),$$

613 where $t_0 > 0$ is a fixed constant, and Ψ , Φ are defined in (3.5) and (3.7), respectively.
 614 We choose this smooth initial condition so that when we numerically approximate $v_{1,\epsilon}$
 615 in (3.12), the approximation is stable when taking the partial derivatives of $v_{0,\epsilon}$.³
 616 Moreover, we can still obtain a closed-form solution to $v_{0,\epsilon}$ in (3.9),

$$617 \quad (5.2) \quad v_{0,\epsilon}(T, x, y) = \Psi(t_0 + T, x; W_{t_0}^x = 0) \Phi^\dagger(t_0 + T, y).$$

618 For analytical convenience, we further specify $\sigma(x) = \exp(\alpha x)$, where $\alpha > 0$, such
 619 that $\exp(Y)$ follows an exponential OU process. This is also a popular stochastic
 620 volatility model in investment banks. Then we have by direct integration

$$621 \quad (5.3) \quad \langle \sigma \rangle = \int_{-\infty}^{\infty} \frac{\kappa}{\nu\sqrt{2\pi}} \exp\left(\alpha x - \frac{\kappa x^2}{2\nu^2}\right) dx = \exp\left(\frac{\alpha^2 \nu^2}{2\kappa}\right), \quad \langle \sigma^2 \rangle = \exp\left(\frac{4\alpha^2 \nu^2}{2\kappa}\right),$$

622 and

$$623 \quad \langle \sigma(\cdot + U_t) \rangle_\dagger = \exp\left(\frac{\alpha^2 \nu^2 (1 - \rho_y^2)}{2\kappa} + \alpha U_t\right),$$

$$624 \quad \langle \sigma^2(\cdot + U_t) \rangle_\dagger = \exp\left(\frac{4\alpha^2 \nu^2 (1 - \rho_y^2)}{2\kappa} + 2\alpha U_t\right),$$

625

626 where $\langle \cdot \rangle$ denotes as earlier the average over the ergodic distribution of Y , and $\langle \cdot \rangle_\dagger$
 627 over that of Y^\dagger only.

628 As a base case, we choose the parameters $T = 1$, $x_0 = y_0 = 2$, $\mu = 0.05$,
 629 $\rho_x = 0.3$, $\rho_y = 0.2$, $\rho = 0.5$, $\kappa = 0.2$, $\nu = 0.5$, $\alpha = 0.1$, and t_0 in the initial condition
 630 (5.1) as 0.2. We then vary ϵ and estimate the contribution of $v_{0,\epsilon}$ and $v_{1,\epsilon}$ to expected
 631 functionals of the solution. Later on, we will also test the effect of different parameters,
 632 in particular negative ρ , and different ratios of κ and ν .

633 For the computations, we truncate the domain to $[-10, 10] \times [-10, 10]$, chosen
 634 large enough that the effect of truncation with zero Dirichlet boundary conditions on
 635 the solution was found negligible for the tested parameter values.

636 To study the convergence $\epsilon \rightarrow 0$, we consider the linear functional

$$637 \quad (5.4) \quad P_T(v) = \int_0^\infty \int_{-\infty}^\infty v(T, x, y) dy dx, \quad T < \infty.$$

638 There are two motivations for this. First, convergence in distribution of $\mathbb{P}[X_T \in$
 639 $\mathcal{I} | W^x, W^y]$ for intervals \mathcal{I} is theoretically supported by [18] (albeit for the process
 640 with absorption at $x = 0$). Second, P_T models the aggregate loss in credit portfolio
 641 models as e.g. in [4, 3, 16, 18], and is therefore of practical interest.

642 To approximate $P_T(v)$ in (5.4), we use the trapezoidal rule for the numerical
 643 integration.

³If we initialised with Dirac data, further stabilisation may be needed, and the analysis in ℓ_2 would not carry over; see the Fourier analysis in [15, 25] for schemes for simpler SPDEs with Dirac initial data.

644 **5.1. Weak convergence of $P_T(v_{0,\epsilon})$.** We first analyse the numerical conver-
 645 gence of $\mathbb{E}[P_T(v) - P_T(v_{0,\epsilon})]$, where P_T is the functional from (5.4). Since P_T is
 646 linear, we have $P_T(v) - P_T(v_{0,\epsilon}) = P_T(v - v_{0,\epsilon})$. We use the scheme (4.13) to directly
 647 approximate $v - v_{0,\epsilon}$, and estimate $\mathbb{E}[P_T(v - v_{0,\epsilon})]$ by standard Monte Carlo sampling
 648 as detailed below. While simulating $v - v_{0,\epsilon}$ from (3.11), compared to simulating v in
 649 (3.2) and $v_{0,\epsilon}$ in (3.9) separately, lead to the same $\mathbb{E}[P_T(v - v_{0,\epsilon})]$ for $h_x, h_y, k \rightarrow 0$,
 650 the former choice has computational savings and is hence faster by a constant factor.⁴
 651 Given M Brownian paths, the Monte Carlo estimator for $\mathbb{E}[P_T(v - v_{0,\epsilon})]$ is

$$652 \quad \Delta \hat{P}_0 = \frac{1}{M} \sum_{i=1}^M P_T(\tilde{V}_0^{(i)}),$$

653 where $\tilde{V}_0^{(i)}$ is the numerical solution to $v - v_{0,\epsilon}$ for the i -th path of (W^x, W^y) in (4.13).

654 For each ϵ , the numerical error between $\Delta \hat{P}_0$ and $\mathbb{E}[P_T(v - v_{0,\epsilon})]$ consists of
 655 discretisation error in h and k (bias), and Monte Carlo noise (variance). If $h, k \rightarrow 0$,
 656 and $M \rightarrow \infty$, $\Delta \hat{P}_0$ is expected to converge to $\mathbb{E}[P_T(v - v_{0,\epsilon})]$, and we treat $\Delta \hat{P}_0$ as
 657 the weak error in ϵ for small h, k and large M .

658 Figure 1(a) shows the convergence to zero of $\Delta \hat{P}_0$, with $\epsilon = 0.1 \times 2^{-3}, 0.1 \times$
 659 $2^{-4}, \dots, 0.1 \times 2^{-7}$, and error bars with 3 standard deviations. For each ϵ , we let
 660 $h_x = h_y = 2^{-l}$, and $k = 0.5 \cdot 4^{-l}$, where $l = 1, 2, 3, 4$. We use $M = 10^6$ for $l = 1, 2$,
 661 and $M = 10^5$ for $l = 3, 4$, as the computational cost for finer meshes is large. For
 662 $l = 4$ with $M = 10^5$, the run time of the Matlab code is up to around 72 hours with
 663 36 cores in parallel (speed 2300 RPMs, RAM 768GB, Linux system). We take the
 664 results from $l = 4$ as numerical approximation to $\mathbb{E}[P_T(v - v_{0,\epsilon})]$, shown as the black
 665 solid line in the loglog plot in Figure 1(a). One can identify from the figure that
 666 the slope is slightly less than 1/2 (see the dashed line), and linear regression gives a slope
 667 of 0.4237. A plausible reason is that for $l = 4$ the error in h and k is not small enough
 668 to be neglected. We deduce empirically that the weak error $\mathbb{E}[P_T(v - v_{0,\epsilon})]$ is $O(\sqrt{\epsilon})$.

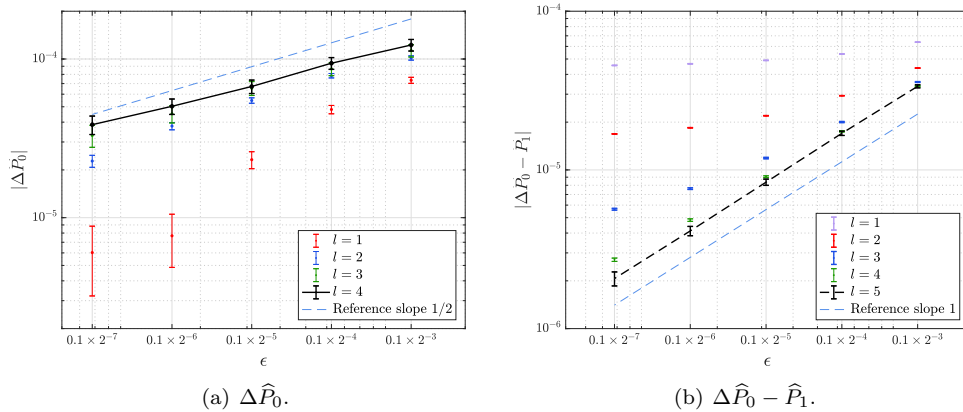


FIG. 1. Weak convergence of $\Delta \hat{P}_0$ and $\Delta \hat{P}_0 - \hat{P}_1$.

⁴Using the same Brownian paths for v and $v_{0,\epsilon}$ leads to a variance reduction and less paths are needed.

669 **5.2. Weak convergence of first order approximation.** To verify $P_T(v_{1,\epsilon})$
 670 is indeed the leading order approximation to $P_T(v) - P_T(v_{0,\epsilon})$, we further exhibit
 671 $\Delta\widehat{P}_0 - \widehat{P}_1$, which is the Monte Carlo estimator for $P_T(v - v_{0,\epsilon} - v_{1,\epsilon})$. Note that we
 672 have used the same Brownian paths for $\Delta\widehat{P}_0$ and \widehat{P}_1 to reduce the variance.

673 Figure 1(b) shows the loglog plot of the convergence of $\mathbb{E}[\Delta\widehat{P}_0 - \widehat{P}_1]$ to zero, with
 674 respect to ϵ , with the error bars being three standard deviations away. Similar to
 675 previous tests, here we stop at $l = 5$ with 1000 Monte Carlo samples, and linear
 676 regression yields a fitted slope of 1.0092.

677 We can thus deduce empirically that $P_T(v_{1,\epsilon})$ is the leading order approximation
 678 to $P_T(v - v_{0,\epsilon})$, with $P_T(v - v_{0,\epsilon} - v_{1,\epsilon}) = O(\epsilon)$.

679 **5.3. Convergence of $\mathbb{E}[P_T(v_{1,\epsilon})]$.** We now analyse $\mathbb{E}[P_T(v_{1,\epsilon})]$, where $v_{1,\epsilon}$ sat-
 680 isfies the SPDE (3.12), and compare it to $P_T^x(v_1^x)$, where v_1^x is the solution to the
 681 marginal SPDE (3.15), and $P_T^x(\cdot)$ is defined by

$$682 \quad P_T^x(v^x) = \int_0^\infty v^x(T, x) dx, \quad T < \infty.$$

683 We expect these two values should be approximately the same.

684 From the derivation of the SPDE for v_1^x in Section 3.4, when we integrate over
 685 the y -dimension in (3.14), we replace $\Phi^Y(T, y)$ in the analytic solution (3.10) by
 686 the invariant distribution $\Phi_\infty^Y(y)$, which yields a more concise analytical form. This
 687 does not change the convergence order, as for $\epsilon \rightarrow 0$, $\Phi^Y(T, y)$ converges to $\Phi_\infty^Y(y)$
 688 exponentially fast. Hence, to make sure $P_T(v_{1,\epsilon})$ gives the same results as $P_T(v_1^x)$, we
 689 also use $v_0(T, x, y) = \Psi(T, x)\Phi_\infty^Y(y)$ as the analytic solution for the zero order term
 690 $v_{0,\epsilon}$ in the schemes (4.13) and (4.14).

691 Given M Brownian paths, we define Monte Carlo estimators for $\mathbb{E}[P_T(v_{1,\epsilon})]$ and
 692 $\mathbb{E}[P_T(v_1^x)]$ by

$$693 \quad (5.5) \quad \widehat{P}_1 = \frac{1}{M} \sum_{i=1}^M P_T(V_1^{(i)}), \quad \widehat{P}_1^x = \frac{1}{M} \sum_{i=1}^M P_T((V_1^x)^{(i)}),$$

694 where V_1 obeys the scheme (4.14), and V_1^x the scheme (4.5).

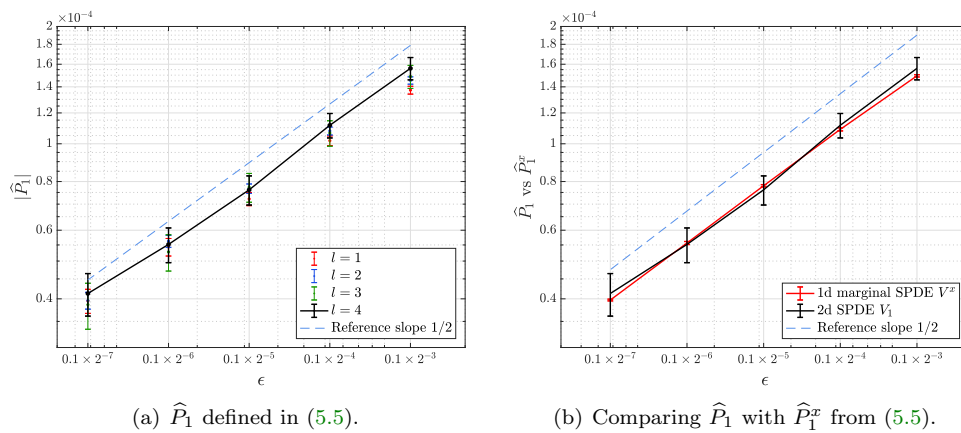


FIG. 2. Weak convergence of \widehat{P}_1 for $h_x = h_y = 2^{-l}$, $k = 0.5 \cdot 4^{-l}$, $\epsilon = 0.1 \times 2^{-3}, \dots, 0.1 \times 2^{-7}$.

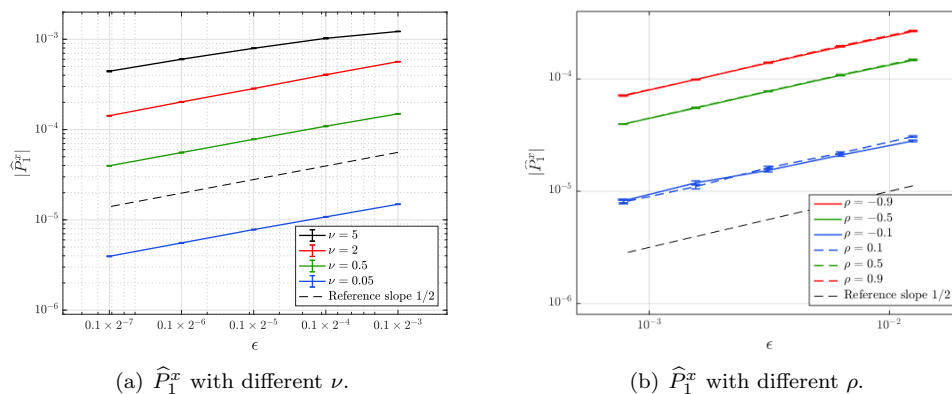
695 Figure 2(a) shows \widehat{P}_1 , with $\epsilon = 0.1 \times 2^{-3}, 0.1 \times 2^{-4}, \dots, 0.1 \times 2^{-7}$, and the
 696 error bars with 3 standard deviations. Similar to Figure 1(a), for each ϵ , we let
 697 $h_x = h_y = 2^{-l}$, and $k = 0.5 \cdot 4^{-l}$, where $l = 1, 2, 3, 4$. We use $M = 10^6$ for $l = 1, 2$,
 698 and $M = 10^5$ for $l = 3, 4$. We take the results from $l = 4$ as numerical approximation
 699 to $\mathbb{E}[P_T(v_{1,\epsilon})]$, shown as the black solid line in the loglog plot in Figure 2(a), comparing
 700 it to a dashed line with slope 1/2.

701 We further include the approximation \widehat{P}_1^x from the marginal SPDE (3.15), and
 702 compare \widehat{P}_1^x with \widehat{P}_1 in Figure 2(b). For \widehat{P}_1^x , we use a multilevel Monte Carlo method,
 703 with prescribed 1% relative error (the ratio between root mean-square error and true
 704 value). We do not give any details on the multilevel construction here (see, e.g.,
 705 [24]), and only note that, unlike approximating $\mathbb{E}[P_T(v)]$ by a standard Monte Carlo
 706 method, and discretising with mesh size $h_l = h_0 \times 2^{-l}$ and timestep $k_l = k_0 \times 4^{-l}$,
 707 approximating by MLMC requires a good coupling between fine path and coarse
 708 path. Therefore, when we apply MLMC to estimate $\mathbb{E}[P_T(v_1^x)]$, the timestep is set as
 709 $k_l = k_0 \times \epsilon \times 4^{-l}$, proportional to ϵ .

710 Linear regression yields that the fitted slope for \widehat{P}_1 is 0.4855, and for \widehat{P}_1^x it is
 711 0.4792. This is consistent with the finding from the previous section that inclusion of
 712 the first order term approximately cancels the error of the zero order approximation,
 713 which is of order $\sqrt{\epsilon}$. Moreover, since v_1^x is the solution to a one-dimensional SPDE,
 714 the computational cost is much lower for $\mathbb{E}[P_T(v_1^x)]$ with the same accuracy than for
 715 $\mathbb{E}[P_T(v_{1,\epsilon})]$, which shows the benefit of our asymptotic expansion.

716 **5.4. Parameter studies.** Finally, we test the effect of the ratio between ν and
 717 κ , and of the correlation ρ . Figure 3(a) shows the effect of different ν/κ , by varying
 718 $\nu \in \{0.05, 0.5, 2, 5\}$, while keeping other parameters fixed. We choose the numerical
 719 parameters to ensure that the relative error is below 1%. We can see from Figure 3(a)
 720 that $|\widehat{P}_1^x|$ increases as ν/κ increases. From the raw data we found approximately that
 721 for fixed ϵ , $|\widehat{P}_1^x(\nu/\kappa; \epsilon)| = O(\nu/\kappa)$, which is consistent with the previous tests where
 722 ϵ varies, through the scaling relationship $(\nu/\sqrt{\epsilon})/(\kappa/\epsilon) = \sqrt{\epsilon}\nu/\kappa$. A point to note is
 723 that the values for $\nu = 5$ are negative, whereas the others are positive.

724 Figure 3(b) shows the effect of changing the parameter ρ , where we make sure to
 725 keep the relative error less than 5%. We can see from Figure 3(b) that $|\widehat{P}_1^x|$ increases
 726 as $|\rho|$ increases; inspection of the raw data shows that \widehat{P}_1^x is positive when ρ is positive,
 727 and vice versa. This effect is similar to the asymptotic expansion of the backward
 728 PDE for the stochastic volatility model [9], where the leading order correction term
 729 is proportional to the correlation between the two Brownian motions involved.

FIG. 3. Comparing \widehat{P}_1^x with regard to ν and ρ .

730

REFERENCES

- 731 [1] BAIN, A., AND CRISAN, D. *Fundamentals of Stochastic Filtering*, vol. 3. Springer, 2009.
- 732 [2] BICHUCH, M., AND SIRCAR, R. Optimal investment with transaction costs and stochastic
- 733 volatility part I: Infinite horizon. *SIAM Journal on Control and Optimization* 55, 6 (2017),
- 734 3799–3832.
- 735 [3] BUJOK, K., AND REISINGER, C. Numerical valuation of basket credit derivatives in structural
- 736 jump-diffusion models. *Journal of Computational Finance* 15, 4 (2012), 115–158.
- 737 [4] BUSH, N., HAMBLY, B. M., HAWORTH, H., JIN, L., AND REISINGER, C. Stochastic evolution
- 738 equations in portfolio credit modelling. *SIAM Journal on Financial Mathematics* 2, 1
- 739 (2011), 627–664.
- 740 [5] CONLON, J. G., AND SULLIVAN, M. G. Convergence to Black–Scholes for ergodic volatility
- 741 models. *European Journal of Applied Mathematics* 16, 3 (2005), 385–409.
- 742 [6] COZMA, A. S., AND REISINGER, C. Simulation of conditional expectations under fast mean-
- 743 reverting stochastic volatility models. In *International Conference on Monte Carlo and*
- 744 *Quasi-Monte Carlo Methods in Scientific Computing* (2020), Springer, pp. 223–240.
- 745 [7] FOUQUE, J.-P., AND HU, R. Multiscale asymptotic analysis for portfolio optimization under
- 746 stochastic environment. *Multiscale Modeling & Simulation* 18, 3 (2020), 1318–1342.
- 747 [8] FOUQUE, J.-P., LORIG, M., AND SIRCAR, R. Second order multiscale stochastic volatility
- 748 asymptotics: stochastic terminal layer analysis and calibration. *Finance and Stochastics*
- 749 20, 3 (2016), 543–588.
- 750 [9] FOUQUE, J.-P., PAPANICOLAOU, G., AND SIRCAR, K. R. *Derivatives in financial markets with*
- 751 *stochastic volatility*. Cambridge University Press, 2000.
- 752 [10] FOUQUE, J.-P., PAPANICOLAOU, G., SIRCAR, R., AND SOLNA, K. Multiscale stochastic volatility
- 753 asymptotics. *Multiscale Modeling & Simulation* 2, 1 (2003), 22–42.
- 754 [11] FOUQUE, J.-P., PAPANICOLAOU, G., SIRCAR, R., AND SOLNA, K. Singular perturbations in
- 755 option pricing. *SIAM Journal on Applied Mathematics* 63, 5 (2003), 1648–1665.
- 756 [12] FOUQUE, J.-P., PAPANICOLAOU, G., SIRCAR, R., AND SOLNA, K. *Multiscale stochastic volatility*
- 757 *for equity, interest rate, and credit derivatives*. Cambridge University Press, 2011.
- 758 [13] FUKASAWA, M. Asymptotic analysis for stochastic volatility: martingale expansion. *Finance*
- 759 *and Stochastics* 15 (2011), 635–654.
- 760 [14] GIESECKE, K., SPILIOPOULOS, K., SOWERS, R., AND SIRIGNANO, J. Large portfolio asymptotics
- 761 for loss from default. *Mathematical Finance* 25, 1 (2015), 77–114.
- 762 [15] GILES, M. B., AND REISINGER, C. Stochastic finite differences and multilevel Monte Carlo for a
- 763 class of SPDEs in finance. *SIAM Journal on Financial Mathematics* 3, 1 (2012), 572–592.
- 764 [16] HAMBLY, B., AND KOLLIPOULOS, N. Stochastic evolution equations for large portfolios of
- 765 stochastic volatility models. *SIAM Journal on Financial Mathematics* 8, 1 (2017), 962–
- 766 1014.
- 767 [17] HAMBLY, B., AND KOLLIPOULOS, N. Stochastic PDEs for large portfolios with general mean-
- 768 reverting volatility processes. *arXiv preprint arXiv:1906.05898* (2019).
- 769 [18] HAMBLY, B., AND KOLLIPOULOS, N. Fast mean-reversion asymptotics for large portfolios of

- 770 stochastic volatility models. *Finance and Stochastics* 24, 3 (2020), 757–794.
- 771 [19] HOWISON, S. Matched asymptotic expansions in financial engineering. *Journal of Engineering*
772 *Mathematics* 53 (2005), 385–406.
- 773 [20] KURTZ, T. G., AND XIONG, J. Particle representations for a class of nonlinear SPDEs. *Stochastic*
774 *Processes and their Applications* 83, 1 (1999), 103–126.
- 775 [21] PAPANICOLAOU, A. Nonlinear filters for hidden Markov models of regime change with fast
776 mean-reverting states. *Multiscale Modeling & Simulation* 10, 3 (2012), 906–935.
- 777 [22] PAPANICOLAOU, A., AND SPILIOPOULOS, K. Filtering the maximum likelihood for multiscale
778 problems. *Multiscale Modeling & Simulation* 12, 3 (2014), 1193–1229.
- 779 [23] REISINGER, C. Mean-square stability and error analysis of implicit time-stepping schemes for
780 linear parabolic SPDEs with multiplicative Wiener noise in the first derivative. *Internation-*
781 *al Journal of Computer Mathematics* 89, 18 (2012), 2562–2575.
- 782 [24] REISINGER, C., AND WANG, Z. Analysis of multi-index Monte Carlo estimators for a Zakai
783 SPDE. *Journal of Computational Mathematics* 36, 2 (2018), 202–236.
- 784 [25] REISINGER, C., AND WANG, Z. Stability and error analysis of an implicit Milstein finite difference
785 scheme for a two-dimensional Zakai SPDE. *BIT Numerical Mathematics* 59, 4 (2019), 987–
786 1029.